

Laser Guide Star Adaptive Optics Imaging Polarimetry of Herbig Ae/Be Stars

Marshall D. Perrin^{1,6*}, James R. Graham^{1,6}, Paul Kalas^{1,6}, James P. Lloyd^{2,6},
 Claire E. Max^{3,6}, Donald T. Gavel^{5,6}, Deanna M. Pennington^{3,6}, Elinor L. Gates^{4,6}

¹Astronomy Department, University of California Berkeley, Berkeley CA 94720

²Astronomy Department, California Institute of Technology, 1201 East California Blvd, Pasadena CA 91125

³Lawrence Livermore National Laboratory, 7000 East Avenue, Livermore CA 94550

⁴UCO/Lick Observatories. P.O. Box 85, Mount Hamilton CA 95140

⁵Laboratory for Adaptive Optics, University of California Santa Cruz,
 1156 High Street, Santa Cruz CA 95064

⁶NSF Center for Adaptive Optics, University of California Santa Cruz,
 1156 High Street, Santa Cruz CA 95064

*To whom correspondence should be addressed; E-mail: mperrin@astro.berkeley.edu

We have used laser guide star adaptive optics and a near-infrared dual-channel imaging polarimeter to observe light scattered in the circumstellar environment of Herbig Ae/Be stars on scales of 100-300 AU. We discover a strongly polarized, biconical nebula 10 arcseconds in diameter (6000 AU) around the star LkH α 198, and also observe a polarized jet-like feature associated with the deeply embedded source LkH α 198-IR. The star LkH α 233 presents a narrow, unpolarized dark lane consistent with an optically thick circumstellar disk blocking our direct view of the star. These data show that the lower-mass T Tauri and intermediate mass Herbig Ae/Be stars share a common evolutionary sequence.

Diffraction-limited optical and infrared astronomy from the ground requires adaptive optics (AO) compensation to eliminate atmospheric wavefront disturbances. Bright stars may be used as wavefront references for this correction, but most astronomical targets lack nearby guide stars. AO observations of these targets from the ground can only be accomplished using artificial laser guide stars (LGS) [1].

Herbig Ae/Be stars are young stars with masses between 1.5 and 10 times that of the sun; they are the intermediate-mass counterparts of the more common T Tauri stars. Excess infrared and millimeter emission shows that Herbig Ae/Be stars are associated with abundant circumstellar dust [2]. Visible and near-infrared (NIR) light scattered from dust is typically polarized perpendicular to the scattering plane [3], making polarimetry a useful tool for probing the distribution of this material [4]. While Herbig Ae/Be stars are intrinsically very luminous, many are so distant or extincted that they are too faint to act as their own wavefront references and thus require LGS AO.

The Herbig Ae/Be stars LkH α 198 and LkH α 233 (Table S1) were observed on 2003 July 22 at the 3-m Shane telescope at Lick Observatory (Fig. S1) using the Lawrence Livermore National Laboratory LGS AO system[5] and the Berkeley NIR camera IRCAL[6]. The atmospheric seeing was 0.8 arcseconds at 550 nm, and the AO-corrected wavefront produced images with Strehl ratios \approx 0.05 – 0.1 at 2.1 microns and full-width at half maximum resolution of 0.27 arcseconds [7].

IRCAL's imaging polarimetry mode utilizes a cryogenic LiYF₄ Wollaston prism to produce two simultaneous images of orthogonal polarizations. The sum of the two channels gives total intensity, and the difference gives a Stokes polarization. The dominant noise source near bright stars in AO images is an uncorrected seeing halo. Because this halo is unpolarized and thus vanishes in the difference image, dual-channel polarimetry enhances the

dynamic range in circumstellar environments[8]. The observing techniques and data reduction methods are based on [9].

LkH α 198 is located at the head of an elliptical loop of optical nebulosity extending 40 arcseconds to the star's southeast [10]. This complex region 600 parsecs distant includes a molecular CO outflow [11] and two Herbig-Haro jets [12], as well as two additional Herbig Ae/Be stars in the immediate vicinity (V376 Cas and LkH α 198-IR) [13] and a millimeter source (LkH α 198-MM) believed to be a deeply embedded protostar [14]. This proximity of sources requires high resolution observations to disentangle the relationships between the various components[15]. We discover a biconical nebula \sim 10 arcseconds in diameter (6000 AU), oriented north-south, with polarization vectors concentric with respect to LkH α 198 (Fig. 1). The lobes of the reflection nebula are divided by a dark, unpolarized lane that we interpret as a density gradient towards the equatorial plane of a circumstellar disk and/or a flattened envelope. The north-south orientation indicates that LkH α 198 is unlikely to have created the giant elliptical nebula or the molecular outflow to the southeast. However, it is consistent with LkH α 198 being the source for the Herbig-Haro flow at a position angle (PA, measured east from north) of 160° , a conclusion supported by the extension of the polarized reflection nebula along this PA. However, this is 20° away from the observed symmetry axis of the nebula, requiring an inner disk axis tilted or precessing with respect to the outer envelope.

The embedded source LkH α 198-IR [16] is detected in our H and K_s band data 5.5 arcseconds from LkH α 198 at PA= 5° . A polarized, extremely blue, jet-like feature extends >2 arcseconds (1200 AU) from LkH α 198-IR at PA= 105° [17]. The polarization vectors of this apparent jet are perpendicular to its long axis, indicating that LkH α 198-IR is the illuminating source, not LkH α 198. The jet appears to be half of a parabolic feature opening toward the southeast, with its apex at LkH α 198-IR and its southern side partially obscured by the envelope around LkH α 198. We suggest that the northwest side of a bipolar structure around LkH α 198-IR may be hidden at NIR wavelengths by the dust indicated by millimeter observations [18]. The orientations of circumstellar structures revealed by our images confirm that LkH α 198-IR is the best candidate for the origin of the Herbig-Haro outflow to PA 135° , though based on geometrical considerations we cannot entirely exclude the protostar LkH α 198-MM. By extension, the large elliptical nebula was most likely created by outflow from LkH α 198-IR, although we see it primarily in scattered light from the optically much brighter LkH α 198.

LkH α 233 is an embedded A5e-A7e Herbig Ae/Be star which is associated with a blue, rectangular reflection nebula 50 arcseconds in extent, located in the Lac OB1 molecular cloud at 880 parsecs. Our imaging polarimetry reveals four distinct lobes bisected by a narrow, unpolarized lane with PA $\approx 150^\circ$ (Fig. 1). The nebulosity around LkH α 233 is extremely blue in the NIR, with its east-west extent decreasing from 6 arcseconds (5300 AU) at J and H to 2 arcseconds (1800 AU) at K_s . The orientation of the lobes relative to the dark lane suggests that they are the limb-brightened edges of a conical cavity in a dusty envelope illuminated by a highly extincted star. The radial extent of the dark lane (1000 AU) suggests that it is associated with an equatorial torus characteristic of a flattened infalling protostellar cloud [19], and not a rotationally-supported disk.

We find that the intensity peak of the star is shifted southwest relative to the polarization centroid, with the displacement increasing from 0.15 arcseconds at K_s to 0.35 arcseconds at J . This too indicates that the lane consists of optically thick foreground material which has a flattened spatial distribution consistent with a circumstellar disk or infalling protostellar cloud. We do not see the star directly, but instead view a scattering surface above the disk midplane.

Our results are consistent with low-resolution, wide-field optical imaging polarimetry[20], which suggests a circumstellar torus in the northwest-southeast direction perpendicular to a bipolar reflection nebula. Our interpretation is also consistent with the existence of an optical [S II] emission line jet [21] blue-shifted to the southwest. The jet both bisects the nebulosity and lies perpendicular to the proposed disk. The geometry of the reflection nebula indicates that the outflow is only poorly collimated ($\Delta\theta \approx 70^\circ$) despite the apparently narrow jet traced by optical forbidden line emission. Because [S II] line emission arises preferentially in regions denser than the critical density for this transition, the surface brightness distributions can take on the appearance of a highly collimated jet, despite the fact that the streamlines collimate logarithmically slowly [22].

Observations of T Tauri stars have led to a general understanding of the origin of solar-type stars [23]: The fragmentation and collapse of an interstellar cloud creates a self-gravitating protostar surrounded by a Keplerian accretion disk fed by an infalling, rotationally-flattened envelope. The disk mediates the outflows common to low-mass young stellar objects, which play a key role in the dispersal of the natal gas and dust.

It has been hypothesized that the more massive Herbig Ae/Be stars and the T Tauri stars form and evolve in

similar manners [24], but this remains controversial. On large spatial scales, the disk-like nature of the circumstellar matter around Herbig Ae/Be stars is well established. Flattened structures around several sources have been resolved on 100 AU scales [25], or have Keplerian kinematics [26]. However, the evidence seems to be ambiguous on scales of tens of AU and below, with some authors arguing for a spherical geometry [27] and others favoring disks [28].

LkH α 198 and LkH α 233 are both classified as Hillenbrand Group II Herbig Ae/Be stars: they have infrared spectra that are flat or rising towards longer wavelengths. This means that they are young stars that may or may not possess circumstellar disks but do possess circumstellar envelopes which are not confined to a disk plane. We observe such envelopes around both of our sources in the form of centrosymmetrically polarized biconical nebulosities viewed approximately edge-on to the midplanes.

We compared our observations with radiative transfer models computed for a sequence of circumstellar dust distributions around T Tauri stars [29, 30]. These models provide both total and polarized intensity images, which we convolved with a model instrumental point spread function to match our observed resolution (Fig. S2). Bipolar outflow cavities in these models produce a limb-brightened appearance at near-infrared wavelengths, with the brightening stronger in polarized light than in total intensity.

For both LkH α 233 and LkH α 198, the peak polarization differs between the two lobes. These asymmetries may indicate the sign of the inclination of each object. In Whitney’s model envelopes, which use dust grain properties fit to an extinction curve for the Taurus molecular cloud, the closer lobe was brighter overall but had lower fractional polarization by several percent. For LkH α 198, the polarization in the northern lobe of the bipolar nebulosity is generally 10-15% lower than the southern lobe at all wavelengths (20% vs. 35% at H , for instance), suggesting that the northern lobe is oriented towards us. For LkH α 233, the southwest lobe is 14% polarized on average versus 26% for the northeast lobe. This indicates that the southern lobe is facing us, consistent with the the blueshift of the CO jet in that direction, and the southwest shift of the intensity peak relative to the polarization centroid.

LkH α 233’s limb-brightened appearance provides compelling evidence for the presence of cavities swept out by bipolar outflow from the star. Cavity models with an opening angle of 30-40° seen at an inclination of 80° reproduce both the observed polarization fraction of 25-40% and the higher degree of limb brightening seen in the near lobe.

The absence of limb brightening may be evidence that LkH α 198 lacks polar cavities, or at most possesses very narrow ones. The detectability of limb brightening for a given angular resolution depends on the opening angle between the symmetry axis and edge of the cavity. At our resolution, envelope models with cavity opening angles greater than $\sim 20^\circ$ predict detectable limb brightening, while we observe for LkH α 198 an opening angle of 45° without limb brightening. Thus our observations do not support the presence of evacuated cavities in the envelope of LkH α 198. The observed morphology can instead be explained by the illumination of a cavity-free, rotationally-flattened envelope by the central star; the bipolar appearance would then arise from light escaping along the path of least optical depth. However, these cavity-free infalling envelope models have opening angles which increase with wavelength, while we observe a constant opening angle, suggesting a geometric rather than optical depth origin for the observed morphology. This discrepancy may be resolvable by varying the dust particle properties.

Based on these observations, LkH α 233 is the more evolved of the two systems, with well-defined cavities swept out by bipolar outflow and bisected by a very dark lane. LkH α 198 is a less evolved system, which is only in the early stages of developing bipolar cavities and possesses lower extinction in the apparent disk midplane.

The observed circumstellar environments are consistent with the rotationally-flattened infall envelopes models developed for T Tauri stars, indicating that the process of envelope collapse has similar phases, despite the large disparities in mass and luminosity between these two classes of young stars. This morphological similarity leads us to infer that the conservation and transport of angular momentum is the dominant physical process for both classes of stars. Alternate formation pathways have been suggested for OB stars that invoke new physical mechanisms, such as magnetohydrodynamic turbulence [31] or stellar mergers [32]. The Herbig Ae stars studied here appear to be below the mass threshold at which such effects become important.

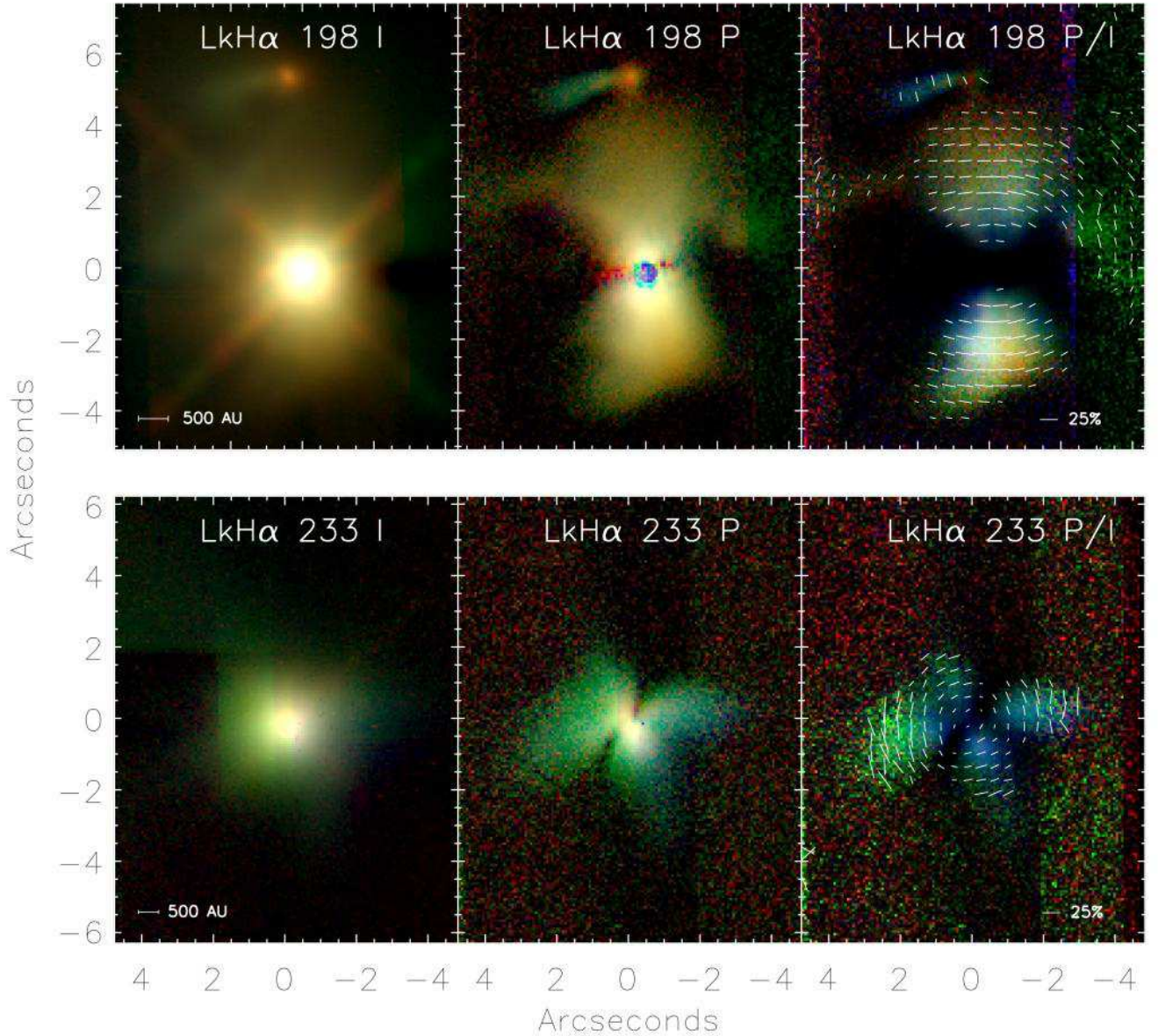


Figure 1: Three-color LGS AO mosaics of LkH α 198 and LkH α 233. Plotted from left to right for each object are the total intensity (Stokes I), the polarized intensity ($P = \sqrt{Q^2 + U^2}$) and the polarization fraction (P/I). I and P are displayed using log stretches, while P/I is shown on a linear stretch. Red is K_s band (2.1 microns), green H (1.6 microns), and blue J (1.2 microns). Polarization vectors for H band are overplotted on the P/I image; while the degree of polarization changes somewhat between bands, the position angles do not vary much. Integration times per band were 960 s and 1440 s for LkH α 198 and LkH α 233, respectively. The dimmest circumstellar features detected in our polarimetric observations are approximately $1 - 2 \times 10^4$ fainter than the stellar intensity peaks. The IRCAL polarimeter is sensitive to polarization fractions as low as a few percent, resulting in a signal-to-noise ratio of 5-10 per pixel for the typical polarizations of 15-40% observed around our targets.

LGS AO Imaging Polarimetry of Herbig Ae/Be Stars Supporting Online Material

Methods and Materials

The Lick Adaptive Optics system was developed at Lawrence Livermore National Laboratory, and can operate in both natural and laser guide star modes [5, 33]. In the laser guide star mode, the atmospheric wavefront reference is created by a laser tuned to the sodium D2 line at 589 nm, which excites mesospheric sodium at roughly 90 km altitude. The 589 nm light is generated by a tunable dye laser pumped by a set of frequency-doubled solid-state (Nd:YAG) lasers. Typically, 11-14 W of average laser power is projected into the sky with a pulse width of 150 ns and a pulse repetition rate of 13 kHz. Laser guide star systems are insensitive to tip and tilt, requiring a separate tip/tilt sensor using a natural guide star. For the observations presented here, the science targets served as their own tip/tilt references.

The sodium guide star has an apparent size of ~ 2 arcseconds in 1 arcsecond seeing and a magnitude which depends on the atmospheric sodium density, which varies on all timescales from hourly to seasonally. The sodium level was low during July 2003, decreasing the magnitude of the guide star, and forcing the adaptive optics system to operate at its lowest frame rate of 55 Hz. As a result, the Strehl ratios achieved were modest ($S \sim 0.05-0.1$) despite the good atmospheric seeing. Correspondingly the full-width at half-maximum (FWHM) of the point spread function was larger than the FWHM of a diffraction limited beam, 0.27 arcseconds versus 0.15 arcseconds respectively at 2.1 microns.

The science camera used with the Lick AO system is IRCAL [6], which has as its detector a 256^2 pixel HgCdTe PICNIC array manufactured by Rockwell. The observations presented in this paper used the standard astronomical J (1.24 micron), H (1.65 micron), and K_s (2.15 micron) broad-band filters. IRCAL's plate scale, 0.0754 arcsec/pixel, was chosen to Nyquist sample the diffraction-limited beam at K_s . The imaging polarimetry mode of IRCAL utilizes a cryogenic LiYF_4 (frequently called "YLF") Wollaston prism to produce simultaneous images of orthogonal polarizations. YLF was chosen for its excellent achromaticity throughout the near infrared. A rotating achromatic half-wave plate mounted immediately before the camera entrance window modulates the polarization, allowing measurement of both Stokes parameters Q and U .

Each target was observed for the same amount of time in J , H , and K_s , divided equally between Stokes Q and U observations. Typical exposures were 30-90 s in duration, with small dithers performed every few exposures. Total integration time was 1440 s per band for $\text{LkH}\alpha$ 233, and 960 s per band for $\text{LkH}\alpha$ 198. The data were flat-fielded and bias-subtracted in the standard manner for near infrared astronomical data. Sky background frames were obtained in polarimetric mode and subtracted from the data. However, the near infrared sky is nearly unpolarized so this step is not essential. The data from different dither positions were registered together via a Fourier transform cross-correlation code and stacked to produce mosaic Stokes I , Q , and U images. These observing techniques and data reduction methods are based on [9].

The instrumental polarization bias was established through observations of standard stars known to be unpolarized; From the derived bias ($\sim 2\%$ at a position angle of -85°) we calculate the effective Mueller polarization matrix for the instrument and apply the inverse of this matrix to the Stokes mosaics to remove the bias.

Table 1: Target Summary

Object	V (magnitudes)	Distance (parsec)	Spectral Type	Luminosity (L_{\odot})	Mass (M_{\odot})	Time per band (s)
LkH α 198	14.3	600	A5e-A7e	5.6	1.2	960
LkH α 233	13.6	880	A5e	28.2	2.6	1440

V magnitude, distance, luminosity, and mass are from [2].



Figure 2: The Lick Observatory LGS AO system in operation on 2003 July 22. The laser beam is visible in Rayleigh scattered light for several kilometers. The faint cirrus clouds illuminated by the Moon remained outside our pointing direction and did not interfere with the observations. The yellowish cast of the dome is due to the street lights of nearby San Jose.

References and Notes

- [1] W. Happer, G. J. MacDonald, C. E. Max, F. J. Dyson, *Optical Society of America Journal* **11**, 263 (1994).
- [2] L. A. Hillenbrand, S. E. Strom, F. J. Vrba, J. Keene, *Astrophys. J.* **397**, 613 (1992).
- [3] P. Bastien, *Astrophys. J.* **317**, 231 (1987).
- [4] D. A. Weintraub, A. A. Goodman, R. L. Akeson, *Protostars and Planets IV* pp. 247–271 (2000).
- [5] C. Max, *et al.*, *Science* **277**, 1649 (1997).
- [6] J. P. Lloyd, *et al.*, *Proc. SPIE Vol. 4008, p. 814-821, Optical and IR Telescope Instrumentation and Detectors, Masanori Iye; Alan F. Moorwood; Eds.* (2000), vol. 4008, pp. 814–821.
- [7] Additional information on materials and methods is available as supporting material on Science Online.
- [8] D. E. Potter, *et al.*, *Astrophys. J.* **540**, 422 (2000).
- [9] J. R. Kuhn, D. Potter, B. Parise, *Astrophys. J. Lett.* **553**, L189 (2001).
- [10] W. Li, N. J. Evans, P. M. Harvey, C. Colome, *Astrophys. J.* **433**, 199 (1994).
- [11] J. Canto, L. F. Rodriguez, N. Calvet, R. M. Levreault, *Astrophys. J.* **282**, 631 (1984).
- [12] D. Corcoran, T. P. Ray, P. Bastien, *Astron. Astrophys.* **293**, 550 (1995).
- [13] R. Hajjar, P. Bastien, *Astroph. J.* **531**, 494 (2000).
- [14] G. Sandell, D. A. Weintraub, *Astron. Astrophys.* **292**, L1 (1994).
- [15] C. D. Koresko, P. M. Harvey, J. C. Christou, R. Q. Fugate, W. Li, *Astrophys. J.* **485**, 213 (1997).
- [16] P. O. Lagage, *et al.*, *Astrophys. J. Lett.* **417**, L79+ (1993).
- [17] M. Fukagawa, *et al.*, *Pub. Astron. Soc. Japan* **54**, 969 (2002).
- [18] T. Henning, A. Burkert, R. Launhardt, C. Leinert, B. Stecklum, *Astron. Astrophys.* **336**, 565 (1998).
- [19] S. Terebey, F. H. Shu, P. Cassen, *Astrophys. J.* **286**, 529 (1984).
- [20] C. Aspin, M. J. McCaughrean, I. S. McLean, *Astron. Astrophys.* **144**, 220 (1985).
- [21] M. Corcoran, T. P. Ray, *Astron. Astrophys.* **336**, 535 (1998).
- [22] F. Shu, *et al.*, *Astrophys. J.* **429**, 781 (1994).
- [23] F. H. Shu, F. C. Adams, S. Lizano, *Ann. Rev. Astron. Astrophys.* **25**, 23 (1987).
- [24] F. Palla, S. W. Stahler, *Astron. J.* **418**, 414 (1993).
- [25] V. Mannings, A. I. Sargent, *Astrophys. J.* **490**, 792 (1997).
- [26] V. Mannings, D. W. Koerner, A. I. Sargent, *Nature* **388**, 555 (1997).
- [27] J. di Francesco, N. J. Evans, P. M. Harvey, L. G. Mundy, H. M. Butner, *Astrophys. J.* **432**, 710 (1994).
- [28] A. Natta, *et al.*, *Astron. Astrophys.* **371**, 186 (2001).
- [29] B. A. Whitney, K. Wood, J. E. Bjorkman, M. J. Wolff, *Astrophys. J.* **591**, 1049 (2003).
- [30] B. A. Whitney, K. Wood, J. E. Bjorkman, M. Cohen, *Astrophys. J.* **598**, 1079 (2003).

- [31] C. F. McKee, J. C. Tan, *Astrophys. J.* **585**, 850 (2003).
- [32] I. A. Bonnell, M. R. Bate, H. Zinnecker, *Mon. Not. R. Astron. Soc.* **298**, 93 (1998).
- [33] D. T. Gavel, *et al.*, *Proc. SPIE Vol. 4494*, p. 336-342, *Adaptive Optics Systems and Technology II*, Robert K. Tyson; Domenico Bonaccini; Michael C. Roggemann; Eds. (2002), pp. 336–342.
34. We are indebted to the Lick Observatory staff who assisted in these observations, including Tony Misch, Kostas Chloros, and John Morey, and also to the many individuals who have contributed to making the laser guide star system a reality. We thank Barbara Whitney for providing us with electronic versions of her models. Onyx Optics fabricated our YLF Wollaston prisms. This work has been supported in part by the National Science Foundation Science and Technology Center for Adaptive Optics, managed by the University of California at Santa Cruz under cooperative agreement No. AST-9876783; and also under the auspices of the U.S. Department of Energy, National Nuclear Security Administration by the University of California, Lawrence Livermore National Laboratory under contract No. W-7405-Eng-48. PK received additional support from the NASA Origins Program under grant NAG5-11769. MDP is supported by a NASA Michelson Graduate Fellowship, under contract to the Jet Propulsion Laboratory (JPL). JPL is managed for NASA by the California Institute of Technology.

Supporting Online Material

www.sciencemag.org
Materials and Methods
Table S1
Figures S1, S2